Orion revisited. II. The foreground population to Orion A

H. Bouy, J. Alves, E. Bertin, L. M. Sarro, D. Barrado

▶ **To cite this version:**

H. Bouy, J. Alves, E. Bertin, L. M. Sarro, D. Barrado. Orion revisited. II. The foreground population to Orion A. Astronomy and Astrophysics - A&A, 2014, 564, 10.1051/0004-6361/201323191 . insu-03645678

HAL Id: insu-03645678

https://insu.hal.science/insu-03645678

Submitted on 24 Apr 2022

HAL is a multi-disciplinary open access archive for the deposit and dissemination of scientific research documents, whether they are published or not. The documents may come from teaching and research institutions in France or abroad, or from public or private research centers.

L'archive ouverte pluridisciplinaire **HAL**, est destinée au dépôt et à la diffusion de documents scientifiques de niveau recherche, publiés ou non, émanant des établissements d'enseignement et de recherche français ou étrangers, des laboratoires publics ou privés.

A&A 564, A29 (2014)
DOI: 10.1051/0004-6361/201323191
© ESO 2014

Astronomy & Astrophysics

Orion revisited⋆,⋆⋆

II. The foreground population to Orion A

H. Bouy[1], J. Alves[2], E. Bertin[3], L. M. Sarro[4], and D. Barrado[1]

[1] Centro de Astrobiología, INTA-CSIC, Depto Astrofísica, ESAC Campus, PO Box 78, 28691 Villanueva de la Cañada, Madrid, Spain
e-mail: hbouy@cab.inta-csic.es
[2] Department of Astrophysics, University of Vienna, Türkenschanzstrasse 17, 1180 Vienna, Austria
[3] Institut d'Astrophysique de Paris, CNRS UMR 7095 UPMC, 98bis Bd Arago, 75014 Paris, France
[4] Dpto. de Inteligencia Artificial, ETSI Informática, UNED, Juan del Rosal, 16, 28040 Madrid, Spain

Received 4 December 2013 / Accepted 31 January 2014

ABSTRACT

Aims. Following the recent discovery of a large population of young stars in front of the Orion nebula, we carried out an observational campaign with the DECam wide-field camera covering ≈10 deg^2 centered on NGC 1980 to confirm, probe the extent of, and characterize this foreground population of pre-main-sequence stars.
Methods. We used multiwavelength wide-field images and catalogs to identify potential foreground pre-main-sequence stars using a novel probabilistic technique based on a careful selection of colors and luminosities.
Results. We confirm the presence of a large foreground population towards the Orion A cloud. This population contains several distinct subgroups, including NGC 1980 and NGC 1981, and stretches across several degrees in front of the Orion A cloud. By comparing the location of their sequence in various color–magnitude diagrams with other clusters, we found a distance and an age of 380 pc and 5 ∼ 10 Myr, in good agreement with previous estimates. Our final sample includes 2123 candidate members and is complete from below the hydrogen-burning limit to about 0.3 $M_\odot$, where the data start to be limited by saturation. Extrapolating the mass function to the high masses, we estimate a total number of ≈2600 members in the surveyed region.
Conclusions. We confirm the presence of a rich, contiguous, and essentially coeval population of about 2600 foreground stars in front of the Orion A cloud, loosely clustered around NGC 1980, NGC 1981, and a new group in the foreground of the OMC-2/3. For the area of the cloud surveyed, this result implies that there are more young stars in the foreground population than young stars inside the cloud. Assuming a normal initial mass function, we estimate that between one to a few supernovae must have exploded in the foreground population in the past few million years, close to the surface of Orion A, which might be responsible, together with stellar winds, for the structure and star formation activity in these clouds. This long-overlooked foreground stellar population is of great significance, calling for a revision of the star formation history in this region of the Galaxy.

Key words. stars: formation – stars: massive – stars: pre-main sequence – ISM: clouds – ISM: individual objects: Orion A

1. Introduction

The Orion star-forming complex is the nearest active star-forming region to Earth that produces massive stars, and is one of the richest in the nearest 1-kpc. It has long been recognized as a benchmark laboratory for star and planet formation studies as well as for the formation and dispersal of OB associations. The entire Orion star formation complex spreads across 200 pc and has spawned about 10^4 stars in the past 12 Myr (e.g. Brown et al. 1994; Bally 2008; Muench et al. 2008; Briceno 2008). There are at least four subpopulations of young stars within the complex, first identified by Blaauw (1964), from the older and dust-free Orion OB 1a group in the North (age ∼10 Myr) to the still-embedded Orion OB 1d (age ∼1 Myr), or the Orion nebula cluster (ONC), to the South. It was realized early that the groups Orion OB 1c and 1d overlapped, at least in part, along the line of sight (e.g. Warren & Hesser 1978; Gomez & Lada 1998).

Recently, Alves & Bouy (2012) used the denser regions of the Orion A cloud to block the background light in the optical, effectively isolating the stellar population in front of it, and found a rich stellar population in front of this cloud. The surprising result in this paper was not the confirmation of the existence of a foreground population, but how rich this population is, in particular towards the previously unstudied NGC 1980 cluster, which was shown to be slightly older (∼5 Myr) than the embedded population in the cloud and contains a full stellar spectrum from OB stars to substellar objects. Using X-ray observations, Pillitteri et al. (2013) recently found a population of sources towards the Orion A cloud that shows a very low amount of extinction (on the order of $N_{\rm H} = 3 \times 10^{20}$ cm^{-2}, or about 0.1 mag of visual extinction) towards ι-Ori and NGC 1980. This very low extinction population coincides with the foreground population isolated in Alves & Bouy (2012), further confirming its presence. The existence of a rich foreground population implies that the closest massive star formation and cluster formation benchmark, namely the ONC (e.g. Da Rio et al. 2012), suffers from significant foreground contamination (on the order of 10% for the ONC, but higher for the less rich L1641 young population). This result also implies that massive star-forming regions can

⋆ Appendix A is available in electronic form at http://www.aanda.org
⋆⋆ Full Table A.1 is only available at the CDS via anonymous ftp to cdsarc.u-strasbg.fr (130.79.128.5) or via http://cdsarc.u-strasbg.fr/viz-bin/qcat?J/A+A/564/A29

have complex star formation histories, and superposition of distinct young populations along a given line of sight probably is the norm, which complicates the determinations of, for example, the stellar yield of a molecular cloud, the duration of the star formation process (age spreads), and mass functions.

Alves & Bouy (2012) made a first estimation of the size of the population (about 2000 objects) by extrapolating from the relatively high extinction regions of Orion A to a larger field. This estimate was necessarily approximate, and called for a better characterization of the foreground population. In the current paper we make use of data from a dedicated observational campaign with the DECam wide-field camera, covering about 10 square degrees of sky centered on NGC 1980, to confirm, probe the extent of, and characterize the foreground population.

This paper is structured as follows: in Sect. 2 we describe the observational data acquired for this project as well as the archival data used. In Sect. 3 we present the results of our approach, namely the identification of the two foreground populations and their characterization. We present a general discussion on the importance of the result found in Sect. 4 and summarize our main results in Sect. 5.

2. Data

To characterize the foreground population to the Orion A molecular cloud we made use of existing surveys together with raw data from Cerro Tololo Inter-American Observatory (CTIO) and its new wide-field Dark Energy Camera (DECam).

2.1. CTIO/DECam

The Orion A cloud was observed at the CTIO with the DECam wide-field camera on the Blanco telescope in the Sloan *griz* and *Y* filters on 2012 October 30 and November 19, 20, and 22 (P.I. Bertin & Bouy) during the science verification of the instrument. Figure 1 gives an overview of the area covered by these observations. The conditions were clear. The full width at half maximum (FWHM) measured in the images oscillated between 0.9–2.″3. These numbers are indicative only because the point spread function (PSF) was sometimes very elongated and highly asymmetric. DECam images where indeed obtained while the instrument was still being tested, and suffered from tracking problems in some parts of the sky, leading to variable amounts of PSF elongation and distortions. This problem was eventually fixed soon after our observations were completed. Sets of short, intermediate, and long exposures were obtained in each filter, as described in Table 1. The individual raw images were processed using an updated version of *Alambic* (Vandame 2002), a software suite developed and optimized for the processing of large multi-CCD imagers, and adapted for DECam. *Alambic* includes standard processing procedures such as overscan and bias subtraction for each individual readout port of each CCD, flat-field correction, bad-pixel masking, and CCD-to-CCD gain harmonization. DECam is only moderately affected by fringes even in the reddest filters, with fringe amplitudes <1% (DES consortium, priv. comm.), and no fringe correction was attempted here. Aperture and PSF photometry were extracted from the individual images using SExtractor (Bertin & Arnouts 1996) and PSFEx (Bertin 2011). The individual catalogs were then registered and aligned on the same photometric scale using Scamp (Bertin 2006). The photometric zero-points of the merged catalog were derived by cross-matching with the Sloan Digital Sky Survey III DR9 catalog (SDSS DR9, Ahn et al. 2012) for the *griz* filters, and with the UKIDSS catalog (Lawrence et al. 2007) for the *Y* filter. The DECam observations typically reach a 3σ completeness limit of 23 ∼ 24 mag and complement the SDSS and UKIDSS catalogs in their faint end and around the bright Orion nebula region that is lacking in both the SDSS and UKIDSS data.

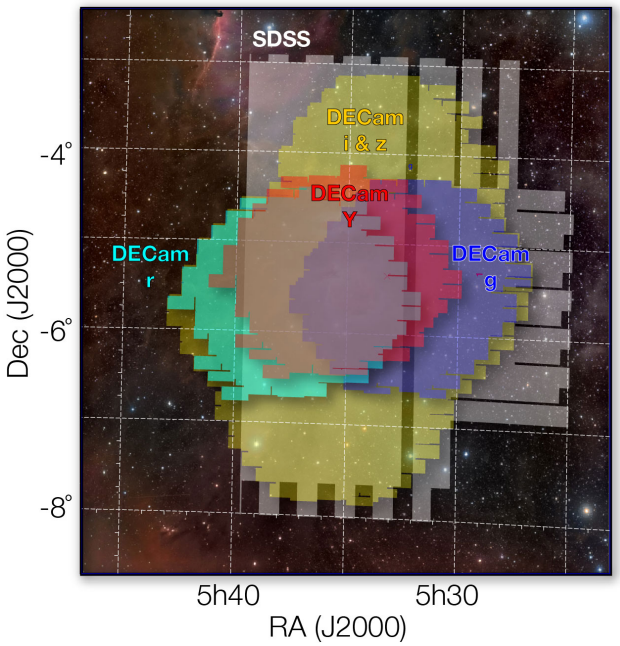

Fig. 1. Coverage of the SDSS and DECam images used in this study. The white area corresponds to the SDSS survey. The blue, cyan and red areas correspond to the DECam *g*, *r* and *Y*-band observations, respectively. The yellow area was observed with DECam in the *i* and *z* bands. Background photograph courtesy of Rogelio Bernal Andreo (DeepSkyColors.com).

Table 1. CTIO/DECam observations.

Filter	Exposure time (s)
g	3,90
r	20, 90
i	3, 30, 90
z	3, 30, 90
Y	30

2.2. Public catalogs

We retrieved the astrometry and photometry for all sources within a box slightly larger than the DECam survey and encompassing the region between 82.°6 < RA < 85.°0 and −7.°6 < Dec < −3.°8 in the SDSS DR9 catalog, 2MASS catalog (Skrutskie et al. 2006), UKIDSS catalog, and APASS catalog (Henden et al. 2009). Table 2 gives a summary of the filters used for these catalogs.

3. Results: a pre-main-sequence population in front of the Orion A association

3.1. General considerations

Figure 2 shows a *r* vs. *r* − *i* color–magnitude diagram of the region. A dense redder sequence is immediately identifiable, indicating the presence of a rich co-eval population. The sequence is also identifiable in any other color–magnitude

Table 2. Catalogs and observations used in this study.

Instrument or survey	Band
SDSS (DR9)	*u*,*g*,*r*,*i*,*z*
CTIO/DECam	*g*,*r*,*i*,*z*,*Y*
2MASS	*J*,*H*,*Ks*
UKIDSS (DR10)	*Z*,*Y*,*J*,*H*,*K*s
APASS (DR1)	*B*,*V*,*r*,*i*

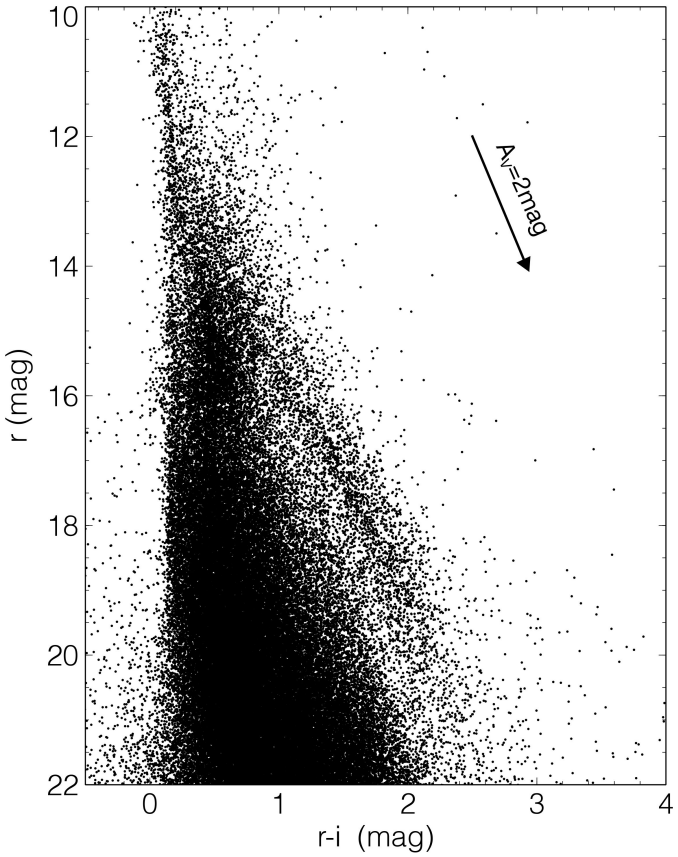

Fig. 2. r vs. $r - i$ color–magnitude diagram including the DECam measurements complemented by SDSS and APASS. An arrow represents an extinction vector of 2 mag.

diagrams that we drew from our dataset. Several basic characteristics can be inferred from this diagram immediately:

- the density of the sequence suggests that the group is rich and massive,
- the sequence appears to be mostly unaffected by reddening, indicating that the group is in front of the Orion A cloud and associations,
- the dispersion of the sequence (less than ≈1 mag) is lower than typically seen for very young (<5 Myr) cluster (Mayne et al. 2007).

3.2. Member selection

Cluster members are traditionally identified based on their location in various color–magnitude diagrams with respect to theoretical or empirical isochrones. This method suffers from several limitations. Because the color–magnitude diagrams are analyzed sequentially, any member with partial photometric measurements will be missed. Additionally, this method does not quantify the membership probability of a given source. In this study, we selected members using a novel multidimensional probabilistic analysis using carefully selected color–magnitude diagrams and luminosities. The method is described in detail in Sarro et al. (2014). Briefly, an initial training set is obtained through the following steps. First a simple ad hoc cut in the r versus $r - i$ diagram of sources (with measurements available in all the g, r, i, z, Y, H, and K bands) yields a subset of sources with a probability density dominated by cluster members. Then, a multivariate Gaussian distribution is fit to this subset and sources at Mahalanobis[1] distances (from its mean) greater than three are removed from the set. Finally, a principal curve (Hastie & Stuetzle 1989) is fit to the resulting dataset in the multidimensional color–magnitude space spanned by $r, z, H, (r - i), (i - K)$, and $(g - i)$. At the same time, a mixture-of-Gaussians model is fit to the remaining set of field/background sources, comprising those below the linear cut in the r vs. $(r - i)$ diagram and those at Mahalanobis distances above three (in the same multidimensional color–magnitude space). The complexity of the mixture-of-Gaussians model is determined by the optimal Bayesian information criterion (BIC) value. From that point onward, an expectation-maximization iterative scheme is applied, whereby in each cycle we

i) first compute the expected membership probability of sources according to these two models (mixture-of-Gaussians for the field and a principal curve for the cluster members), and then
ii) we modify the membership list accordingly (removing low-probability sources and adding high-probability ones), and infer a new principal curve model that accounts for the changes.

New high-probability members (defined here conservatively as having a probability ≥99.75%) are then selected as the new training set, while originally selected members with a lower probability are rejected from the training set. The calculation takes into account measurement uncertainties on the photometry, as well as data censoring. This is particularly important since the various datasets combined in our study have very different coverage (Fig. 1) and depths (Table 1). The method leads to 2123 high-confidence (probability ≥ 99.5%) cluster members among the 605 020 sources of our initial catalog. Figure 3 illustrates the results and shows the sequence obtained in two color–magnitude diagrams.

Members of coincident background young associations (such as those in the ONC) most likely contaminate the final sample. Assuming that the young population associated with the ONC and the Orion A cloud suffers from extinction higher than about $A_V \sim 1$ mag, a conservative assumption, a simple independent test on how severe this contamination might be is to search for reddened sources in a sensitive near-infrared (NIR) color–color diagram. We found that of the selected sample, only about 1–2% of the sources showed NIR colors indicating $A_V > 1$ mag, which gives additional confidence to our selection procedure.

Our selection process is, regardless, expected to give a lower contamination rate and a more complete list of members than the traditional method described above. As illustrated in Fig. 3, the selection method works best in the luminosity range where the cluster sequence is clearly separated from the background/foreground population. We expect the resulting sample

[1] The Mahalanobis distance provides a relative measure of a data point's distance from a reference in a multidimensional space.

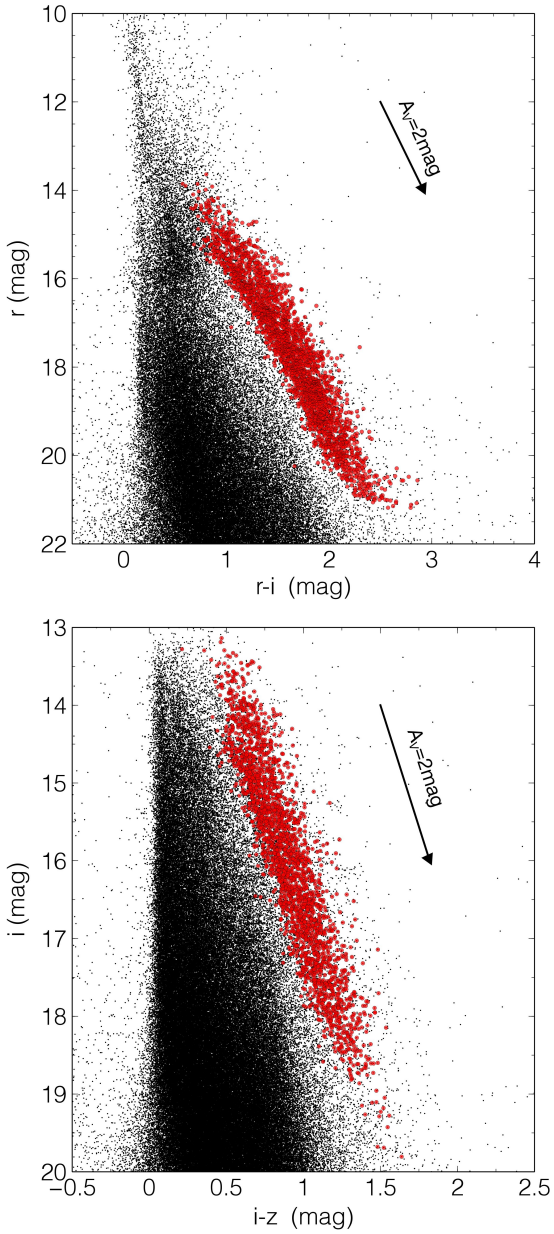

Fig. 3. r vs. $r - i$ (*upper panel*) and i vs. $i - z$ (*lower panel*) color–magnitude diagrams of the survey. Objects with a membership probability ≥99.5% are represented with red dots.

to be mostly complete in the luminosity range between $15 \lesssim r \lesssim 19.5$ mag and $14.5 \lesssim i \lesssim 17.5$ mag.

3.3. Spatial distribution and origin

Figure 4 shows the spatial distribution of candidate members with a membership probability higher than 99.5% (hereafter OriA-foreground). The sources cluster around several known groups: NGC 1980, NGC 1981, L1641W, and L1641N. An overdensity is also visible southwest of OMC 3 on one hand, and at the position reported by Chupina & Vereshchagin (2000) for Group 189 in both X-ray and optical source density maps on the other hand.

NGC 1980 and NGC 1981 belong to a foreground population, as demonstrated by Alves & Bouy (2012) and Maia et al. (2010), respectively. Although we cannot rule out that L1641W is associated to the Orion A cloud, we note that both its projected distance away from the cloud and its age suggest that it belongs to the foreground population. The overdensity located on top of L1641N could be produced by genuine L1641N members. The low extinction towards these sources (as found in the NIR color–color diagram) and the small fraction of stars with mid-infrared excess nevertheless suggest that it could be a distinct population. It is not possible to draw firm conclusions and we consider the distance and origin of this group undetermined and to be confirmed.

The overdensity of sources southwest of OMC3 does not correspond to any group previously identified in the literature, and we hereafter refer to it as OriA-Fore 1. It does not appear in the X-ray source density map of Alves & Bouy (2012) because it falls near the edge of the field covered by the *XMM-Newton* observations. Figure 5 shows a *Spitzer* [3.6] – [4.5] vs. [5.8] – [8.0] color–color diagram for sources located within 20′ from the centroid of the overdensity. ONC and OMC2/3 members from the literature are also represented for comparison. This diagram produces an excellent diagnostic to easily distinguish between objects with and without disks. The vast majority of the OriA-Fore 1 sources show no or little excess, indicating a more advanced evolutionary status than their ONC or OMC2/3 counterparts, and suggesting that they are a distinct population.

Interestingly, Alves & Bouy (2012) found a velocity dispersion for sources located in the vicinity of OriA-Fore 1 (see their Fig. 8) significantly different from those of the ONC and NGC 1980 (23.3 ± 3.0 km s^{-1} for the group that falls on top of the dense gas in OMC2 and 27.5 ± 2.3 km s^{-1} for the new group, to the West of OMC2). The errors are too large and the samples relatively small so that we cannot draw a strong conclusion, but both the spatial distribution and velocity dispersion are suggestive of two overlapping populations. Approximately 70 sources are located within 10′ of the centroid, and 162 within 20′. The absence of bright massive OB stars in this area and the low luminosity of the sources ($14 \leq i \leq 18$ mag) suggest that the group forms a low-mass cluster. The current datasets do not allow us to draw a firm conclusion on its distance. Its location away from the cloud, the low disk-frequency, and the distinct velocity dispersion suggest that the group is not directly associated to the Orion A.

3.4. Age and distance

Pre-main-sequence (PMS) fitting uses the positions of stars in color–magnitude diagrams to derive ages and distances to young star clusters. Instead of fitting the cluster's PMS with theoretical isochrones that can be uncertain at young ages (Baraffe et al. 2009), we derived relative ages and distances by comparing the observed PMS with the empirical PMS of well-known clusters.

3.4.1. Comparison of NGC 1980 and NGC 1981

To minimize the contamination by OMC 2/3, L1641N (and possibly L1641W and OriA-Fore 1, if they belong to Orion A), we isolated high-probability members of NGC 1980 and NGC 1981 by selecting sources located within 20′ of their respective centers (Table 3). Figure 6 shows that the two populations are indistinguishable in both a r vs. $(r - H)$ and a i vs. $(i - Ks)$ color–magnitude diagrams, suggesting that they have very similar ages and distances. Maia et al. (2010) reported a distance of 380 ± 17 pc, a reddening of $E(B-V) = 0.07 \pm 0.03$ mag, and an age of 5 ± 1 Myr for NGC 1981, which places the foreground population $10 \sim 40$ pc in front of the Orion A cloud.

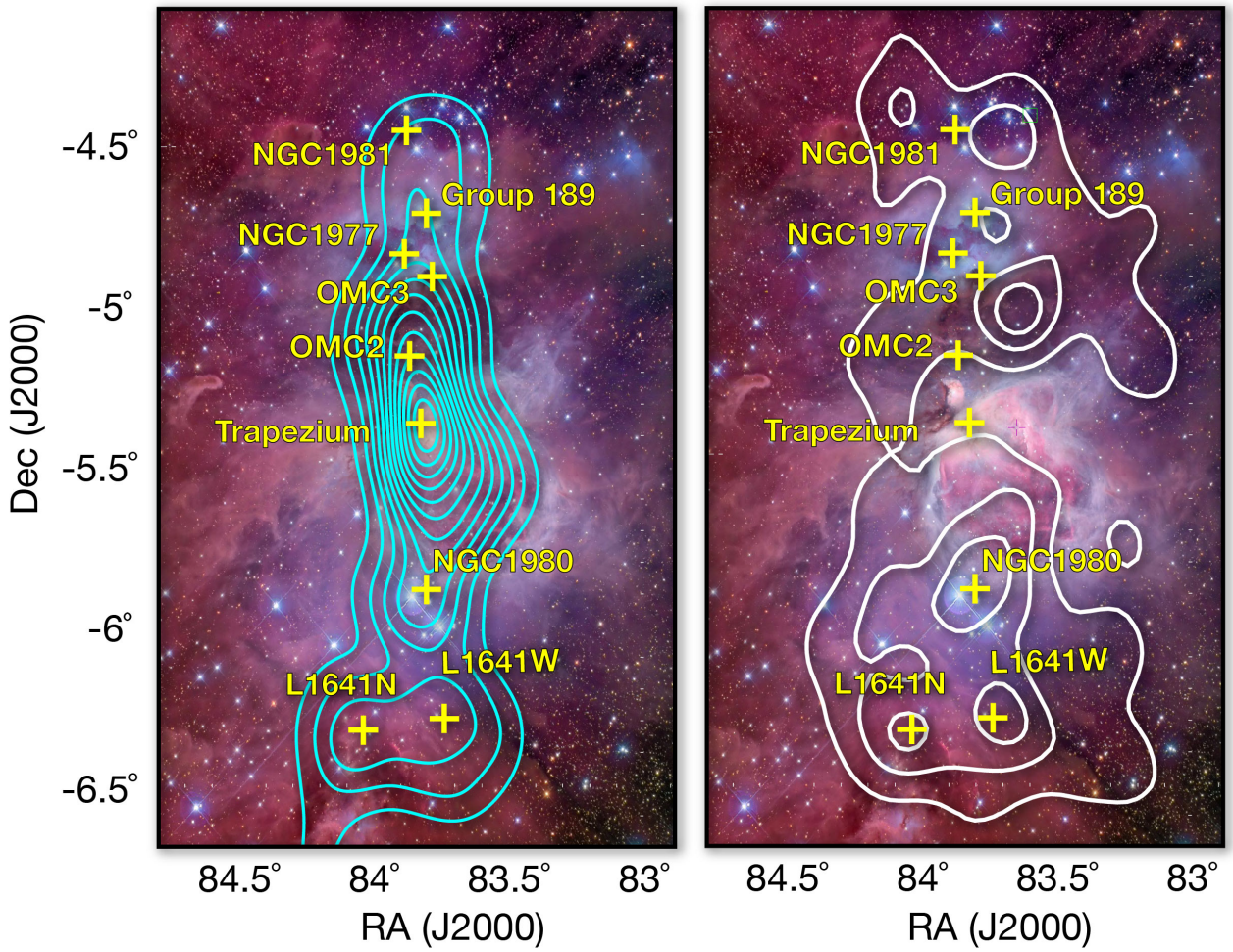

Fig. 4. *Left*: contours of the spatial density distribution of X-ray sources from Alves & Bouy (2012). *Right*: contours of spatial density distribution of optically selected candidate members of the foreground population (this work). Background photograph courtesy of Jon Christensen (christensenastroimages.com).

Table 3. Orion groups and clusters.

Name	RA (J2000)	Dec (J2000)	Age (Myr)	Distance (pc)	Reference
		Orion A			
NGC 1980	83.°80	−5.d95	5 ~ 10	~380	(1)
NGC 1981	83.°78	−4.d34	5 ± 1	380 ± 17	(2)
Group 189	83.°84	−4.d71	...	...	(3)
L1641N	83.°94	−6.d28	2 ~ 3	...	(4)
Trapezium	83.°84	−5.d40	1 ~ 3	390 ~ 440	(4), (5), (6)
OMC 2	83.°86	−5.°17	$\lesssim$1	420 ~ 450	(4), (6), (7)
OMC 3	83.°79	−4.°92	$\lesssim$1	420 ~ 450	(4), (6), (7)
L1641W	83.°69	−6.d28	5 ~ 10	~380?	(1)
OriA-Fore 1	83.°62	−4.d97	5 ~ 10	~380?	(1)
		Ori OB1abc & λ−Ori			
Collinder 80	83.°88	−1.d10	1 ~ 7	385	(8)
σ-Ori	84.°69	−2.d60	3 ~ 5	385	(8)
Collinder 69	83.°77	+9.d93	5 ~ 10	400	(9)
25 Ori	81.°19	+1.d85	7 ~ 10	380	(10)

References. (1) This work; (2) Maia et al. (2010); (3) Chupina & Vereshchagin (2000); (4) Gomez & Lada (1998); (5) Hirota et al. (2007); (6) Menten et al. (2007); (7) Peterson & Megeath (2008); (8) Caballero & Solano (2008); (9) Barrado y Navascués et al. (2007); (10) Briceño et al. (2007).

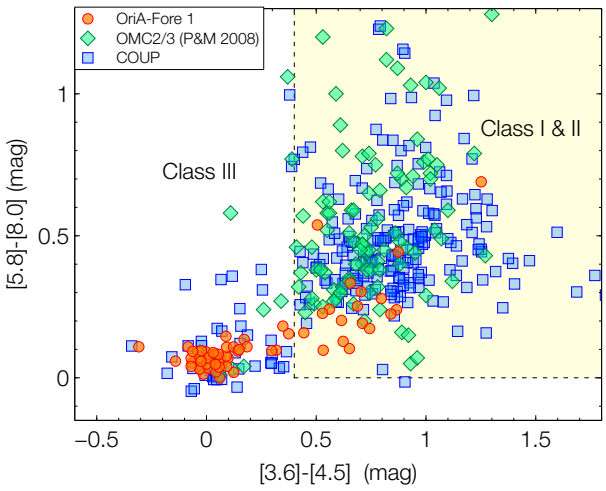

Fig. 5. [3.6] – [4.5] vs. [5.8] – [8.0] color–color diagram for OriA-Fore 1 (orange dots, sources located within 20′ of the centroid of the overdensity, see Fig. 4), for known OMC2/3 members from Peterson & Megeath (2008) (green diamonds) and for the sample of ONC members from the COUP survey (blue squares). Dotted lines represent the boundary between class III and class I & II sources (shaded area) as defined in Allen et al. (2004).

3.4.2. Comparison with Collinder 69

As an independent check, we compared the observed PMS with that of Collinder 69. Collinder 69 is a 5 ∼ 10 Myr cluster located at ≈400 pc in the λ-Orionis star-forming region (Dolan & Mathieu 1999; Barrado y Navascués et al. 2007). Collinder 69 presents several advantages for the purpose of our study. It is well studied and an extensive list of more than 200 spectroscopically confirmed members is available (Bayo et al. 2012). Photometry in almost all the bands presented in the current study has been obtained for its members, making the comparison possible over a broad domain of colors and luminosities. Additionally, it is part of the λ-Orionis star-forming region, a subgroup of the Orion star formation complex (see Fig. 12).

Figure 7 shows a r vs. $(r - H)$ and a i vs. $(i - Ks)$ color–magnitude diagram of the candidate members selected previously with Collinder 69 confirmed members overplotted. Interstellar extinction towards Collinder 69 is relatively low ($A_V \approx 0.37$ mag on average, Diplas & Savage 1994), and we dereddened the photometry accordingly. Extinction towards OriA-foreground is not well established but is expected to be low since it lies in front of the Orion A molecular cloud (Alves & Bouy 2012; Pillitteri et al. 2013; Maia et al. 2010). The match is remarkably good in the two diagrams, especially considering that variability, excesses in the $riHKs$-bands (related to youth, accretion, rotation, and circumstellar disks), and extinction must affect the comparison. We conclude that NGC 1980 and NGC 1981 must have distances and ages similar to Collinder 69, which is consistent with the results of Maia et al. (2010). The comparison of a cluster's PMS with an empirical PMS of differing age would indeed lead to a color-dependent distance modulus, which is not observed here.

3.4.3. Comparison with the ONC

Figure 8 compares the sequence formed by the OriA-foreground population in the same r vs. $(r - H)$ and a i vs. $(i - Ks)$ color–magnitude diagrams with the sequence formed by ONC members selected in the *Chandra* Orion Ultradeep Project (COUP, Getman et al. 2005). The two sequences are clearly different, the COUP sequence is on average brighter in spite of the higher and variable level of extinction that affects the members and the larger distance. The ONC sequence is also much more dispersed, a feature typical of very young (<5 Myr) clusters. These differences can be interpreted as a difference in age and distance, the ONC members being significantly younger than the OriA-foreground population and embedded in the Orion A cloud, in good agreement with the rest of our analysis.

For the rest of the study we consider a distance of 380 pc and an age of 5 ∼ 10 Myr for OriA-foreground.

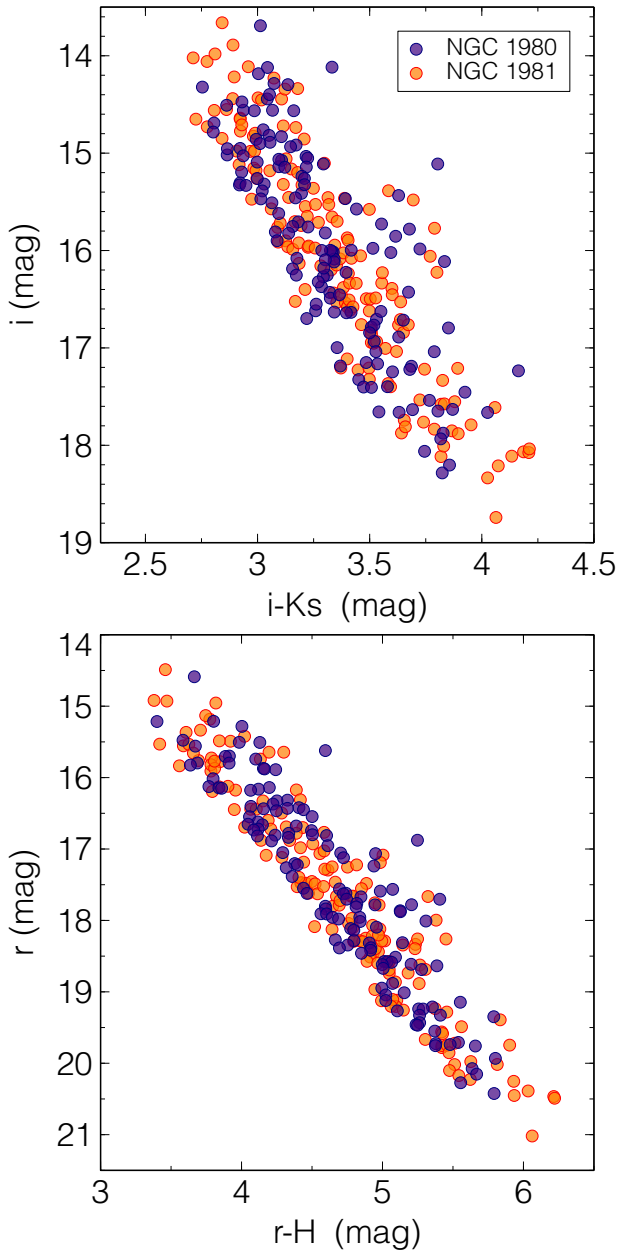

Fig. 6. r vs. $(r-H)$ (*lower panel*) and a i vs. $(i-Ks)$ (*upper panel*) color–magnitude diagrams of sources selected within 20′ of the NGC 1980 (violet) and NGC 1981 (orange) centers.

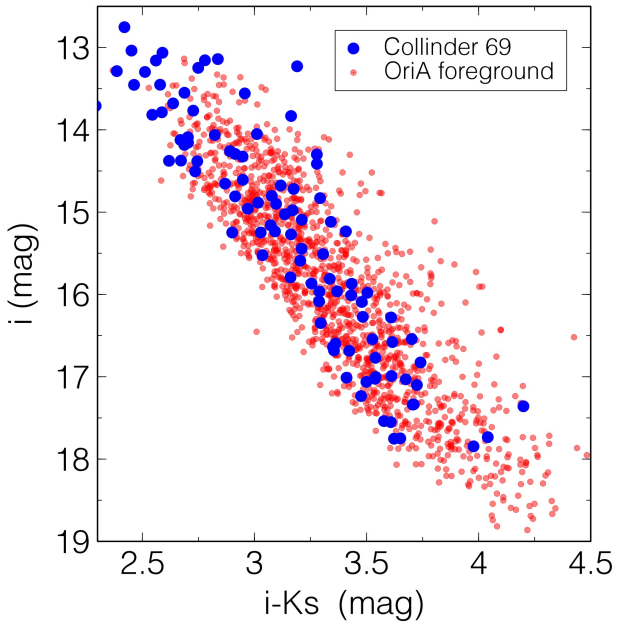

Fig. 7. r vs. $(r-H)$ (*lower panel*) and a i vs. $(i-Ks)$ (*upper panel*) color–magnitude diagrams of OriA-foreground candidate members (red dots) with Collinder 69 confirmed members (blue dots).

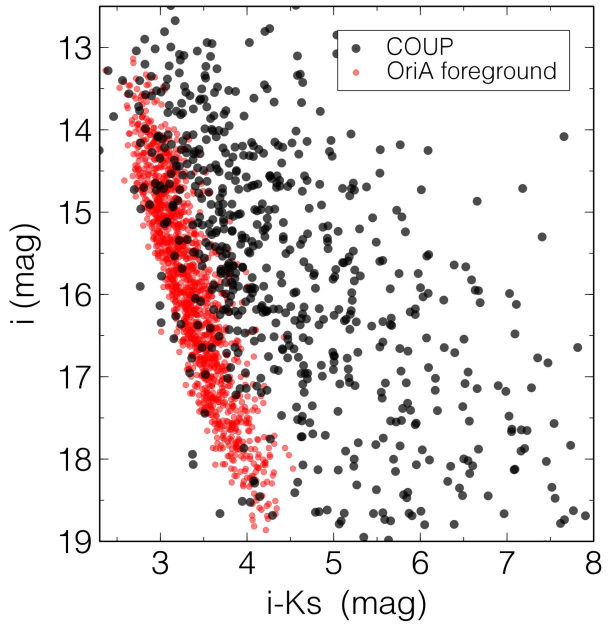

Fig. 8. r vs. $(r-H)$ (*lower panel*) and a i vs. $(i-Ks)$ (*upper panel*) color–magnitude diagrams of OriA-foreground candidate members (red dots), and COUP members of the ONC (black dots).

3.5. Mass function

We estimated the effective temperatures (hereafter $T_{\rm eff}$) of all OriA-foreground candidate members using the virtual observatory SED analyzer (VOSA, Bayo et al. 2008). VOSA offers the advantage of deriving robust $T_{\rm eff}$ independently of the distance and using all the available photometric information instead of a subset of colors and luminosities. The optical and NIR photometry of OriA-foreground candidate members described in Sect. 2 was complemented with *Spitzer* (Alves & Bouy 2012) and WISE (Wright et al. 2010) mid-infrared photometry. Briefly, VOSA compares the observed spectral energy distributions (SED) with a grid of theoretical SEDs based on the BT-Settl models of Allard et al. (2012) and covering the range $2000 < T_{\rm eff} < 5000$ K (by steps of 100 K) and $3.0 < \log\ g < 4.5$ (by steps of 0.5 dex). As mentioned previously, extinction towards OriA-foreground is expected to be low and was neglected. VOSA automatically detects possible excesses from circumstellar disks (in the mid-infrared) or accretion (in the visible and UV), and rejects the corresponding measurements for the fit. The quality and quantity of the photometric measurements (between 4 and 14 measurements per source, with an average of 7 measurements per source) resulted in a robust fit for most sources, as illustrated in Fig. 9. The $T_{\rm eff}$ were then transformed into masses using the ($T_{\rm eff}$ vs. mass) relation given by the BT-Settl models assuming an age of 5 Myr. According to these calculations, the least-massive candidate members have masses of only $\approx$30 $M_{\rm Jup}$, independently of the distance.

The cluster's mass function was then computed over the luminosity range corresponding to the estimated completeness domain of the survey (described in Sect. 3). Figure 10 shows the result. Our survey is essentially complete to M-star masses

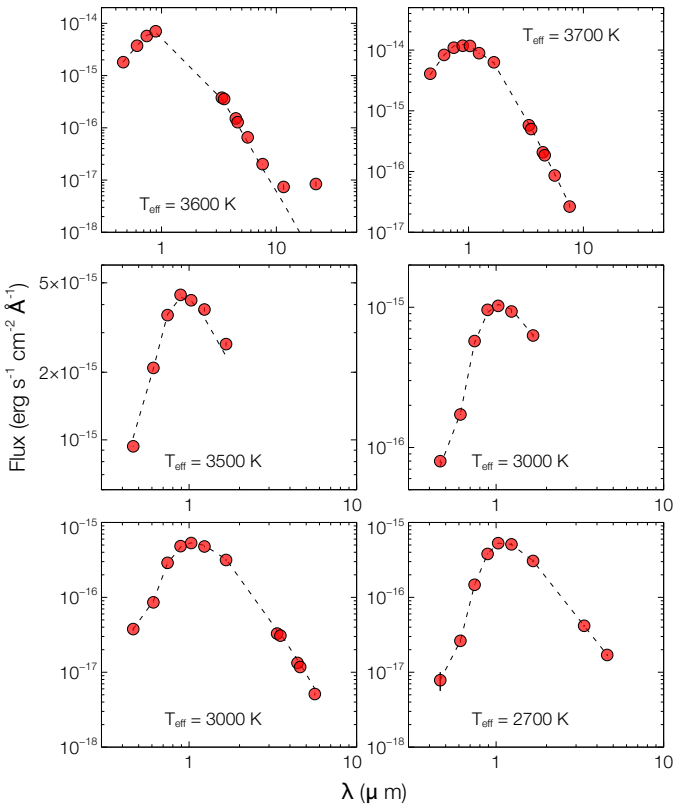

Fig. 9. Examples of SED fitting obtained with VOSA. The red dots represent the observed photometry for a random sample of six sources selected as members. The dashed line represents the best-fit BT-Settl model. The corresponding $T_{\rm eff}$ is indicated.

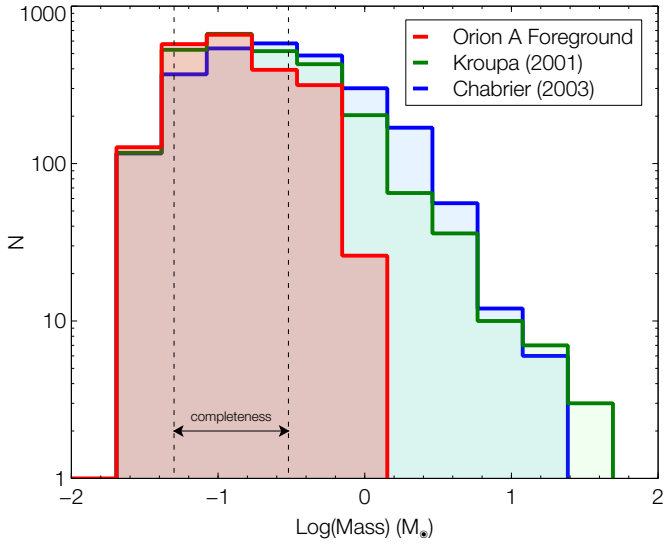

Fig. 10. Mass function of OriA-foreground over the completeness domain computed for 5 Myr and 10 Myr. The predictions of Chabrier (2003) and Kroupa (2001) mass functions are overplotted.

below ~0.3 $M_{\odot}$, down to substellar objects with ~50 $M_{\rm J}$. Extrapolating over the entire mass range using the Chabrier (2003) and Kroupa (2001) mass functions, the total number of members in the cluster is ≈2600. This suggests that we are missing only ≈500 members, most of them massive and beyond the saturation limit of the current data. This value should be regarded as preliminary since a) the current data do not probe the entire area covered by the various groups of OriA-foreground; and b) the member selection suffers from some level of contamination, albeit estimated to be small (~2%). The OriA-foreground population, or Blaauw's OB 1c subgroup, cannot be neglected in understanding the star formation history of the region, and perhaps even the ongoing star formation in Orion A, as we discuss in the next section.

4. Discussion

The present analysis confirms the results of Alves & Bouy (2012) and demonstrates that a large population (≳2600 sources) of 5 ~ 10 Myr stars lies in front of the better known younger Orion A embedded population (e.g. Lada et al. 2000; Megeath et al. 2012). This foreground population is not uniformly distributed, but clusters loosely around the NGC 1980 and NGC 1981 clusters, and possibly also around the recently discovered L1641W (Alves & Bouy 2012) and the newly found OriA-Fore 1 group.

The main result of this paper, the confirmation of a rich ~5 Myr foreground population in the immediate vicinity of the Orion A cloud, fits the general scenario first proposed by Blaauw (1964) and refined by Elmegreen & Lada (1977) well, where the formation of stars in large complexes is not a continuous process, but proceeds sequentially. As already pointed out in Alves & Bouy (2012), this foreground population is not the optical counterpart of the embedded population in Orion A, but a distinct population perhaps responsible for the current star formation in the integral-shaped filament in Orion A (Bally 2008).

As originally proposed by Blaauw (1964), the Orion OB1 association is the product of several sequential star formation events, propagating from the northwest, where the OB1a subgroup is located, towards the belt region (OB1b), and then south towards OB1c (which includes NGC 1980 and NGC 1981), and more recently back towards Orion A in the south, and Orion B east of the Belt stars, the OB1d subgroup (see Bally 2008, for a review). The results presented here suggest that while the overall picture of sequential star formation is not invalidated by our results, there is a higher level of complexity as more star formation subunits present in the region are being discovered. The most intriguing result seems to be that the age of NGC 1980 and NGC 1981, separated by at least 14 pc, is not only indistinguishable within the errors, but is also similar to that of the λ-Ori cluster, located at least 100 pc away. At the same time, and also within the errors, the distance to NGC 1980 and 1981 – or the OB1c subgroup studied here – is similar to the distance of 25-Ori, σ-Ori, λ-Ori, and Collinder 70 clusters, all located at about 380–385 pc (Table 3) and spread across about 100 pc. It is too early to speculate about a 100 pc triggering or synchronization event in Orion, in particular as 25-Ori and OB1a appear to be older than OB1b (e.g Briceño et al. 2007). But it is fair to say that it is not yet clear what the casual relation is between all these star formation events with age differences of only a few to ~5 Myr but spread across about 100 pc of space. Better data are obviously needed to derive better ages and parallaxes, proper motions, and radial velocities to attempt a more refined scenario for the star formation history of the Orion complex.

Regardless of the precise star formation history of Orion, and assuming a normal IMF, a relatively large number of massive stars was formed in the past 10 Myr. Several of these must have already exploded as supernovae, which together with the feedback from the stellar winds from existing stars are shaping the structure of the interstellar medium in the region,

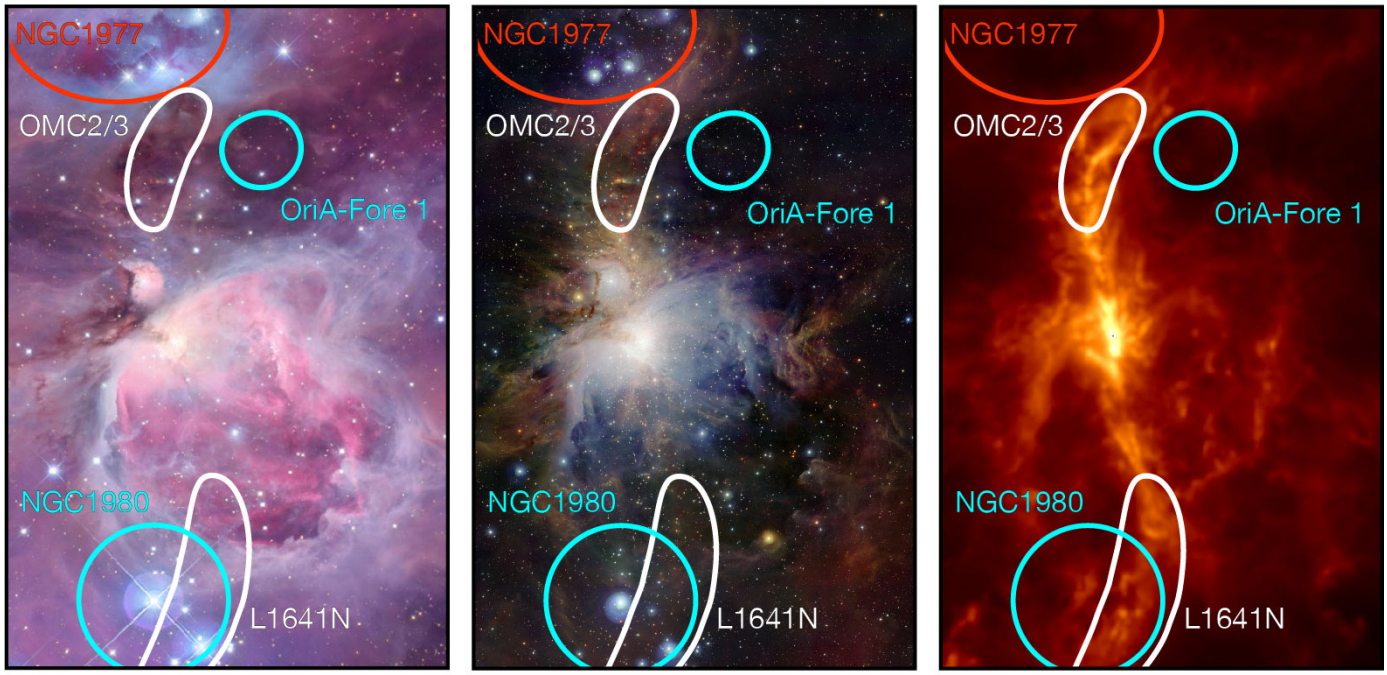

Fig. 11. *From left to right*: optical, near-IR, and far-IR image of the Orion A cloud. Foreground groups are indicated in cyan. Groups associated to Orion A are indicated in white. Group in the back of Orion A are indicated in red. Credits: Jon Christensen (optical); ESO/J. Emerson/VISTA/CASU (near-IR); H. Bouy (Far-IR *Herschel*, SPIRE 500 μm).

including powering the large Barnards loop (O'Dell et al. 2011, see Fig. 12). This feedback process probably compressed the Orion A molecular cloud (located 10–40 pc behind) and triggered the ongoing star formation in the Orion Molecular Cloud, including the ONC, L1641N, and OMC2/3, but also NGC 2024 (and possibly L1641W and OriA-Fore 1).

Figure 11 shows the location of OriA-Fore 1 with respect to the nebulosities and to the cloud. Interestingly, the new group is located inside the northern elbow of the integral-shaped filament, in a region mostly free of dust as probed by *Herschel*, and free of HII nebulosities as probed by the optical. We speculate that the cloud might be squeezed between the massive cluster NGC 1977 in the background, and by the less massive OriA-Fore 1 in the foreground. The compression of the filament between these two groups results in the active star formation in OMC2 and OMC3. Similarly, the strong winds produced by the massive stars of NGC 1980 might be giving its shape to the southern elbow of the integral-shaped filament, and be triggering the star formation in L1641N.

Figure 12 (right panel) shows a schematic representation of the spatial distribution of the various groups on top of a far-infrared map probing the molecular clouds. The most distant and youngest groups all closely follow the cloud. On the other hand, all the closest and older groups but NGC 1980 are located systematically away from the cloud, providing additional evidence that they are not the optical counterpart of the embedded population, but a distinct population, corresponding to a previous star formation episode. The fact that the foreground population to Orion A characterized in this paper generally aligns with the orientation of the Orion A cloud is puzzling and may provide information about the original distribution of molecular gas, but can also be interpreted as a coincidence – surely the reason why so little attention has been dedicated in the literature to this important population.

This scenario provides a simple explanation for the age spread observed in the region (see e.g. Huff & Stahler 2006, and references therein). A fraction of the spread might be purely observational and caused by the contamination from the older coincident foreground population. But most of the age spread is probably real and the result of successively triggered star formation events and consequent episodic bursts of the star formation rate.

5. Conclusions

We combined new wide-field optical observations of the Orion A group of associations with archival data and catalogs. A dense sequence appears clearly in all color–magnitude diagrams. The observed match with empirical sequences suggests an age of 5 ~ 10 Myr and a distance of ≈380 pc, placing the corresponding sources in the immediate front of the Orion A cloud and the ONC. Members of the sequence were selected using a novel multi-dimensional probabilistic analysis using carefully selected color–magnitude diagrams and luminosities. The sources cluster into several groups, which can be spatially associated to NGC 1980, L1641N, L1641W, and NGC 1981, and a new group OriA-Fore 1 located southwest of OMC3. The current work confirms the results reported in Alves & Bouy (2012) using X-ray, optical, and infrared data.

We propose the following scenario to explain the observations in the region: a first generation of clusters and associations located at 380 ~ 400 pc formed between 5 ~ 10 Myr ago. It included NGC 1980, NGC 1981, 25-Ori, σ-Ori, λ-Ori, and possibly L1641W and OriA-Fore 1. These groups formed several thousands of stars, including a few massive stars. After a few million years, the most massive stars must have exploded as supernovae, which together with stellar winds very likely triggered episodic star formation events in the ONC, resulting in

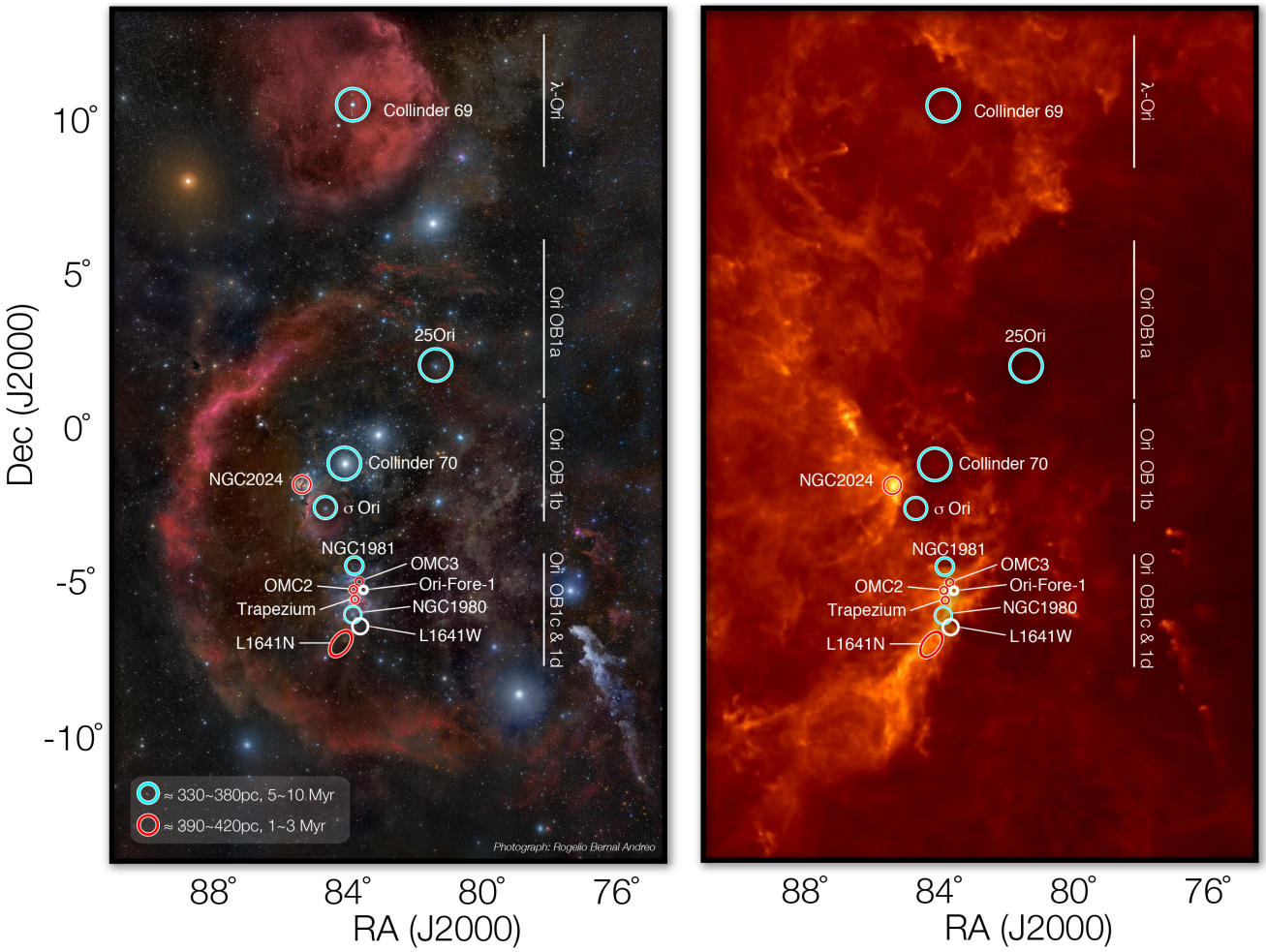

Fig. 12. *Left panel*: distribution of foreground (light blue) and background (red) groups overplotted on an optical photograph of the Orion constellation (courtesy of Rogelio Bernal Andreo – *DeepSkyColors.com*). *Right panel*: same as *left panel*, but overplotted on a far-infrared (850 μm) *Planck* map. L1641W and OriA-Fore 1 distances are uncertain and are represented as a white circles.

the Trapezium, L1641N, OMC2/3, and maybe even NGC 2024 in Orion B.

Acknowledgements. We are grateful to Rogelio Bernal Andreo and Jon Christensen for granting us permission to use their photographs of Orion. H. Bouy is funded by the Spanish Ramón y Cajal fellowship program number RYC-2009-04497. We acknowledge support from the Faculty of the European Space Astronomy Centre (ESAC). This research has been funded by Spanish grants AYA2010-21161-C02-02, AYA2012-38897-C02-01. This publication is supported by the Austrian Science Fund (FWF). We are very grateful to our referee John Bally for a prompt, very useful, and constructive report. We are grateful to the CTIO observers and DECam science verification team, and in particular Dara Norman, for performing the observations. We are grateful to Amelia Bayo for providing us with an electronic version of the Collinder 69 catalog. This research made use of Astropy, a community-developed core Python package for Astronomy (Robitaille et al. 2013). This work has made an extensive use of Topcat (http://www.star.bristol.ac.uk/~mbt/topcat/, Taylor 2005). This research has made use of the VizieR and Aladin images and catalogue access tools and of the SIMBAD database, operated at CDS, Strasbourg, France. This research has made use of VOSA and the Spanish Virtual Observatory. Based on observations obtained with MegaPrime/MegaCam, a joint project of CFHT and CEA/DAPNIA, at the Canada-France-Hawaii Telescope (CFHT) which is operated by the National Research Council (NRC) of Canada, the Institut National des Sciences de l'Univers of the Centre National de la Recherche Scientifique of France, and the University of Hawaii. This research has made use of the APASS database, located at the AAVSO web site. Funding for APASS has been provided by the Robert Martin Ayers Sciences Fund. We are grateful to the AAVSO team for giving us access to the APASS DR1 catalogue. This research is based on data obtained at the Cerro Tololo Inter-American Observatory, National Optical Astronomy Observatory, which are operated by the Association of Universities for Research in Astronomy, under contract with the National Science Foundation. This work is based in part on data obtained as part of the UKIRT Infrared Deep Sky Survey. This research made use of the SDSS-III catalogue. Funding for SDSS-III has been provided by the Alfred P. Sloan Foundation, the Participating Institutions, the National Science Foundation, and the US Department of Energy Office of Science. The SDSS-III web site is http://www.sdss3.org/. SDSS-III is managed by the Astrophysical Research Consortium for the Participating Institutions of the SDSS-III Collaboration including the University of Arizona, the Brazilian Participation Group, Brookhaven National Laboratory, University of Cambridge, University of Florida, the French Participation Group, the German Participation Group, the Instituto de Astrofisica de Canarias, the Michigan State/Notre Dame/JINA Participation Group, Johns Hopkins University, Lawrence Berkeley National Laboratory, Max Planck Institute for Astrophysics, New Mexico State University, New York University, Ohio State University, Pennsylvania State University, University of Portsmouth, Princeton University, the Spanish Participation Group, University of Tokyo, University of Utah, Vanderbilt University, University of Virginia, University of Washington, and Yale University. This publication makes use of data products from the Wide-field Infrared Survey Explorer, which is a joint project of the University of California, Los Angeles, and the Jet Propulsion Laboratory/California Institute of Technology, funded by the National Aeronautics and Space Administration. This research used the facilities of the Canadian Astronomy Data Centre operated by the National Research Council of Canada with the support of the Canadian Space Agency. This publication makes use of data products from the Two Micron All Sky Survey, which is a joint project of the University of Massachusetts and the Infrared Processing and Analysis Center/California Institute of Technology, funded by the National Aeronautics and Space Administration and the National Science Foundation. This work is based in part on observations made with the *Spitzer* Space Telescope, which is operated by the Jet Propulsion Laboratory, California Institute of Technology

under a contract with NASA. This project used data obtained with the Dark Energy Camera (DECam), which was constructed by the Dark Energy Survey (DES) collaborating institutions: Argonne National Lab, University of California Santa Cruz, University of Cambridge, Centro de Investigaciones Energeticas, Medioambientales y Tecnologicas-Madrid, University of Chicago, University College London, DES-Brazil consortium, University of Edinburgh, ETH-Zurich, University of Illinois at Urbana-Champaign, Institut de Ciencies de l'Espai, Institut de Fisica d'Altes Energies, Lawrence Berkeley National Lab, Ludwig-Maximilians Universitat, University of Michigan, National Optical Astronomy Observatory, University of Nottingham, Ohio State University, University of Pennsylvania, University of Portsmouth, SLAC National Lab, Stanford University, University of Sussex, and Texas A&M University. Funding for DES, including DECam, has been provided by the US Department of Energy, National Science Foundation, Ministry of Education and Science (Spain), Science and Technology Facilities Council (UK), Higher Education Funding Council (England), National Center for Supercomputing Applications, Kavli Institute for Cosmological Physics, Financiadora de Estudos e Projetos, Fundação Carlos Chagas Filho de Amparo a Pesquisa, Conselho Nacional de Desenvolvimento Científico e Tecnológico and the Ministério da Ciência e Tecnologia (Brazil), the German Research Foundation-sponsored cluster of excellence "Origin and Structure of the Universe" and the DES collaborating institutions.

References

Ahn, C. P., Alexandroff, R., Allende Prieto, C., et al. 2012, ApJS, 203, 21
Allard, F., Homeier, D., Freytag, B., & Sharp, C. M. 2012, in EAS Pub. Ser. 57, eds. C. Reylé, C. Charbonnel, & M. Schultheis, 3
Allen, L. E., Calvet, N., D'Alessio, P., et al. 2004, ApJS, 154, 363
Alves, J., & Bouy, H. 2012, A&A, 547, A97
Bally, J. 2008, in Overview of the Orion Complex, ed. B. Reipurth, 459
Baraffe, I., Chabrier, G., & Gallardo, J. 2009, ApJ, 702, L27
Barrado y Navascués, D., Stauffer, J. R., Morales-Calderón, M., et al. 2007, ApJ, 664, 481
Bayo, A., Rodrigo, C., Barrado Y Navascués, D., et al. 2008, A&A, 492, 277
Bayo, A., Barrado, D., Huélamo, N., et al. 2012, A&A, 547, A80
Bertin, E. 2006, in Astronomical Data Analysis Software and Systems XV, eds. C. Gabriel, C. Arviset, D. Ponz, & S. Enrique, ASP Conf. Ser., 351, 112
Bertin, E. 2011, in Astronomical Data Analysis Software and Systems XX, eds. I. N. Evans, A. Accomazzi, D. J. Mink, & A. H. Rots, ASP Conf. Ser., 442, 435
Bertin, E., & Arnouts, S. 1996, A&AS, 117, 393
Blaauw, A. 1964, ARA&A, 2, 213
Briceno, C. 2008, in ASP Monograph Publ. 4, ed. B. Reipurth, 838
Briceño, C., Hartmann, L., Hernández, J., et al. 2007, ApJ, 661, 1119
Brown, A. G. A., de Geus, E. J., & de Zeeuw, P. T. 1994, A&A, 289, 101
Caballero, J. A., & Solano, E. 2008, A&A, 485, 931
Chabrier, G. 2003, PASP, 115, 763
Chupina, N. V., & Vereshchagin, S. V. 2000, in Star Formation from the Small to the Large Scale, eds. F. Favata, A. Kaas, & A. Wilson, ESA SP, 445, 347
Da Rio, N., Robberto, M., Hillenbrand, L. A., Henning, T., & Stassun, K. G. 2012, ApJ, 748, 14
Diplas, A., & Savage, B. D. 1994, ApJS, 93, 211
Dolan, C. J., & Mathieu, R. D. 1999, AJ, 118, 2409
Elmegreen, B. G., & Lada, C. J. 1977, ApJ, 214, 725
Getman, K. V., Feigelson, E. D., Grosso, N., et al. 2005, ApJS, 160, 353
Gomez, M., & Lada, C. J. 1998, AJ, 115, 1524
Hastie, T., & Stuetzle, W. 1989, J. Am. Stat. Assoc., 84, 502
Henden, A. A., Welch, D. L., Terrell, D., & Levine, S. E. 2009, BAAS, 41, 669
Hirota, T., Bushimata, T., Choi, Y. K., et al. 2007, PASJ, 59, 897
Huff, E. M., & Stahler, S. W. 2006, ApJ, 644, 355
Kroupa, P. 2001, MNRAS, 322, 231
Lada, C. J., Muench, A. A., Haisch, Jr., K. E., et al. 2000, AJ, 120, 3162
Lawrence, A., Warren, S. J., Almaini, O., et al. 2007, MNRAS, 379, 1599
Maia, F. F. S., Corradi, W. J. B., & Santos, Jr., J. F. C. 2010, MNRAS, 407, 1875
Mayne, N. J., Naylor, T., Littlefair, S. P., Saunders, E. S., & Jeffries, R. D. 2007, MNRAS, 375, 1220
Megeath, S. T., Gutermuth, R., Muzerolle, J., et al. 2012, AJ, 144, 192
Menten, K. M., Reid, M. J., Forbrich, J., & Brunthaler, A. 2007, A&A, 474, 515
Muench, A., Getman, K., Hillenbrand, L., & Preibisch, T. 2008, in ASP Monograph. Publ. 4, ed. B. Reipurth, 483
Robitaille, T. P., Tollerud, E. J., et al., (Astropy Collaboration) 2013, A&A, 558, A33
O'Dell, C. R., Ferland, G. J., Porter, R. L., & van Hoof, P. A. M. 2011, ApJ, 733, 9
Peterson, D. E., & Megeath, S. T. 2008, in ASP Monograph Publ. 4, ed. B. Reipurth, 590
Pillitteri, I., Wolk, S. J., Megeath, S. T., et al. 2013, ApJ, 768, 99
Sarro, L., Bouy, H., Bertin, E., et al. 2014, A&A, 563, A45
Skrutskie, M. F., Cutri, R. M., Stiening, R., et al. 2006, AJ, 131, 1163
Taylor, M. B. 2005, in Astronomical Data Analysis Software and Systems XIV, eds. P. Shopbell, M. Britton, & R. Ebert, ASP Conf. Ser., 347, 29
Vandame, B. 2002, in SPIE Conf. Ser. 4847, eds. J.-L. Starck, & F. D. Murtagh, 123
Warren, Jr., W. H., & Hesser, J. E. 1978, ApJS, 36, 497
Wright, E. L., Eisenhardt, P. R. M., Mainzer, A. K., et al. 2010, AJ, 140, 1868

Page 12 is available in the electronic edition of the journal at http://www.aanda.org

Appendix A: Optical and near-infrared photometry

Table A.1. Astrometry, photometry and membership probability to NGC 1980.

ID	RA (J2000)	Dec (J2000)	g (mag)	r (mag)	i (mag)	z (mag)	Y (mag)	J (mag)	H (mag)	K (mag)	Proba (%)
1	82.215192	–5.46041214899587	17.85 ± 0.06								
2	82.875308	–5.53696629695448	21.43 ± 0.19								
3	82.177325	–5.73258047115825	21.54 ± 0.21								
4	82.884495	–5.69717042076206	16.46 ± 0.06								
5	82.871700	–5.31117868183994	21.59 ± 0.19								
...	...	...	...	...	...	...	...	...	...	...	...
318195	82.8890372	–6.1383945			22.3 ± 0.08	21.78 ± 0.09					0.0
318196	82.8530871	–6.1373586			22.44 ± 0.06	21.89 ± 0.08					0.0
318197	82.7754450	–6.1370855				19.75 ± 0.03					0.0
318198	82.7844997	–6.1369484	23.18 ± 0.13		21.62 ± 0.04	21.36 ± 0.07					0.0
318199	82.6534512	–6.1362583			21.31 ± 0.03	20.68 ± 0.03	19.82 ± 0.16	19.35 ± 0.19			0.0
318200	82.8885940	–6.1364786			21.79 ± 0.04	21.27 ± 0.05					0.0
318201	82.8074845	–6.1360497			22.73 ± 0.09	22.04 ± 0.11					0.0
318202	82.8105568	–6.1356670			22.1 ± 0.05	21.24 ± 0.06					0.0
318203	82.7055493	–6.1350536			22.34 ± 0.05	21.6 ± 0.07					0.0
318204	82.8436510	–6.1352804			21.36 ± 0.03	20.66 ± 0.03		19.12 ± 0.15	18.24 ± 0.18		0.0
318205	82.6438898	–6.1347576	23.77 ± 0.18		20.73 ± 0.03	20.8 ± 0.04	20.23 ± 0.23			17.95 ± 0.17	0.0
...	...	...	...	...	...	...	...	...	...	...	...
132153	84.2702543	–4.2309804	21.39 ± 0.05	19.81 ± 0.02	17.69 ± 0.01	16.49 ± 0.01	15.28 ± 0.0	14.62 ± 0.0	14.12 ± 0.0		100.0
132154	84.2739473	–4.7892626	18.15 ± 0.01	16.73 ± 0.01	15.38 ± 0.01	14.59 ± 0.0					100.0
132155	84.2528004	–5.4169561	17.38 ± 0.01	15.99 ± 0.01	14.54 ± 0.01	13.75 ± 0.0					100.0
132156	83.6885989	–5.2738119		19.63 ± 0.06	17.24 ± 0.02		14.77 ± 0.0	14.16 ± 0.0	13.53 ± 0.04	13.23 ± 0.0	99.9
132157	84.2981832	–6.1125390		18.37 ± 0.05	16.49 ± 0.02			14.04 ± 0.03	13.48 ± 0.0	13.17 ± 0.04	99.9
132158	84.1374590	–6.0416210	18.3 ± 0.07	16.93 ± 0.05	15.49 ± 0.02			13.42 ± 0.03	12.73 ± 0.0	12.48 ± 0.0	99.9
132159	83.7844179	–5.4866692	19.69 ± 0.1	18.6 ± 0.05	16.57 ± 0.02		14.5 ± 0.02	13.82 ± 0.04	13.06 ± 0.03	12.67 ± 0.02	99.9

Notes. The full version is available at the CDS.